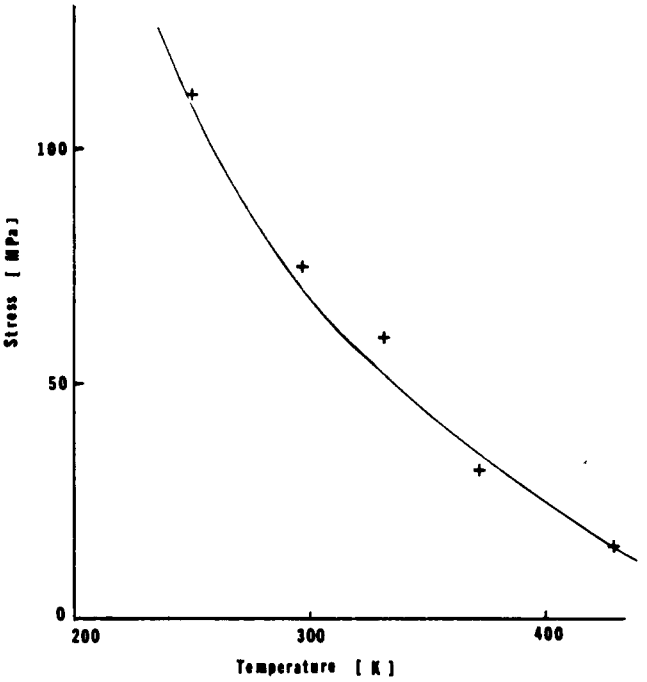

Figure 2. Temperature dependence of the critical stress shown for the onset of the $\alpha \rightarrow \beta$ transition in PBT. The plus signs are taken from the experimental results of ref 2, while the solid curve is a prediction based on the observed hysteresis width reported in the same paper.

with D_1 and D_2 constants.

The fact that the only term in eq 15 that is not linear in T arises directly from the contribution of the hysteresis width ΔS to eq 14 allows us to make a concrete prediction: the curvature of a plot of ΔS with temperature should be exactly twice that of a temperature plot of the critical stress $S^*_{\alpha\beta}$. This prediction is tested in Figure 2, in which the experimental values of Brereton et al.[2] for the critical stress are shown. The solid line represents half the hysteresis width found experimentally in the same study but with a term linear in temperature added to fit the line to the data at the two end points. The agreement is close enough to suggest that the nucleation and growth hypothesis may have some validity.

The values of D_1 and D_2 used to fit Figure 2 yield a value of 1.2 kJ/mol per monomer unit for ΔV. This number is consistent with the requirement that $-SA\Delta L + \Delta V$ be negative for nucleation to occur. Such a requirement places an upper bound on ΔV. The observation that the transition proceeds at room temperature at 75 MPa indicates that $\Delta V < 1.6$ kJ/mol per monomer. This number, incidentally, is considerably less then the value of 25 kJ/mol per monomer suggested by the molecular energy calculation of Yokouchi et al.[7]

We have examined a number of mechanisms that might affect the critical stress and hysteresis width for the $\alpha \rightarrow \beta$ transition in PBT. While contributions to the entropy from changes in phonon frequencies at the transition and internal stresses caused by morphological effects may play some role, they do not appear capable of accounting for the observed temperature dependence of the critical stress. A model of nucleation and growth, on the other hand, appears consistent with the observed data in that a predicted relation between the critical stress and the width of the hysteresis loop is obeyed.

Acknowledgment. We gratefully acknowledge support from the Materials Research Group program of the National Science Foundation through Grant DMR 84-17875.

Registry No. PBT (copolymer), 26062-94-2; PBT (SRU), 24968-12-5.

References and Notes

(1) Datye, V. K.; Taylor, P. L. *Macromolecules* **1985**, *18*, 671.
(2) Brereton, M. G.; Davies, G. R.; Jakeways, R.; Smith, T.; Ward, I. M. *Polymer* **1978**, *19*, 17.
(3) Tashiro, K.; Nakai, Y.; Kobayashi, M.; Tadokoro, H. *Macromolecules* **1980**, *13*, 137.
(4) Stambaugh, B.; Lando, J. B.; Koenig, J. L. *J. Polym. Sci., Polym. Phys. Ed.* **1979**, *17*, 1063.
(5) Menzik, Z. *J. Polym. Sci., Polym. Phys. Ed.* **1975**, *13*, 2173.
(6) Stambaugh, B.; Koenig, J. L.; Lando, J. B. *J. Polym. Sci., Polym. Phys. Ed.* **1979**, *17*, 1053.
(7) Yokouchi, M.; Sakakibara, K.; Chatani, Y.; Tadokoro, M.; Tanaka, T.; Yoda, Y. *Macromolecules* **1976**, *9*, 266.
(8) Merz, W. J. *Phys. Rev.* **1954**, *95*, 690.

Comparing the Flory Approach with the DiMarzio Theory of the Statistical Mechanics of Rodlike Particles

Walter R. Romanko* and Stephen H. Carr

Departments of Chemical Engineering and Materials Science and Engineering and the Materials Research Center, Northwestern University, Evanston, Illinois 60208.
Received August 24, 1987; Revised Manuscript Received November 6, 1987

ABSTRACT: Three descriptions of the rod orientation in the Flory lattice model for rods (generalized to a continuum) are compared in an athermal system with the more accurate DiMarzio model for rodlike particles in a continuum. The Flory-type rod orientation distribution functions yield distributions quite similar to the DiMarzio distribution. The Flory-type distribution function obtained from the rod orientation expression $(y - 1) = (x - 1) \sin \theta$ can be used in the DiMarzio entropy equation at a calculational advantage to yield entropies which are virtually indistinguishable from the original. Flory-type nematic and isotropic entropies differ from the DiMarzio entropies, giving slightly different phase equilibria. A solution to the "entropy catastrophe" for rods is explained in terms of the improper use of a one-dimensional boundary condition in the third dimension.

Introduction

The study of liquid crystals has become quite an important area of research in the past two decades. It is because of certain molecular anisotropies that a fluid displays liquid crystalline properties.[1] One of the simplest shape anisotropies resulting in liquid crystalline order is that of the rigid rodlike molecule or macromolecule. Various approaches of determining the implications of the impenetrability of these particles have been employed to model the thermodynamics of these rigid rodlike particles.

0024-9297/88/2221-2243$01.50/0

The variety of techniques employed have all yielded the same general conclusion: above a critical rod concentration, the shape anisotropy of the rods is sufficient to produce an ordered phase.

Onsager presented a theory in 1949 describing the thermodynamic properties of rodlike particles.[2] His method was based on a virial expansion, truncated at the second term, for rodlike gases. He proved that as a result of the shape anisotropy of the particles, two phases, one isotropic and the other anisotropic, would coexist at certain rod densities (for rods of adequate length). Several other modifications to and approximations of this approach were subsequently introduced.[3-8]

In 1956, Flory used a lattice model to predict the phase relationships of mixtures of rigid rods and spherical solvent molecules.[9] Athermal biphasic equilibria, qualitatively similar to that of Onsager, were calculated to occur for axis ratios greater than 6.7. In the athermal–good-solvent region, the Flory method was shown to follow experimental data better than the Onsager approach. This statistical mechanical representation incorporated a solvent–solute interaction parameter that showed qualitative agreement with experimental data.[10] Several modifications to Flory's lattice model included systems of rods confined to principle-axis directions,[11,12] ensembles possessing continuous distributions of rod angles,[11,13-16] polydisperse systems,[16-22] systems with both stiff and flexible moieties,[23,24] and systems possessing order-dependent energies.[12,15,16,22]

Many other methods of packing rods have been examined. Monte Carlo simulations have been utilized for thermodynamic and orientational studies of rigid rods on a lattice.[25,26] Statistical mechanical approaches differing from that of Flory have been presented.[11,12,27,28] Another technique employed was a lattice–spin field theory that involved cluster expansions for systematic corrections to mean-field theory to give a very accurate statistical description to this abecedarian[29] problem. The Landau theory of phase transitions applied to anisotropic particles also predicts the first-order isotropic–nematic transition.[30]

Flory Lattice Approximations

There have been several discrepancies in the use of the classical lattice model for calculation of the thermodynamic properties of rigid, rodlike macromolecules[13,16,31,32] (as well as for flexible macromolecules). Perhaps the most notable enigma is the "entropy catastrophe",[31,33,34] which occurs when W, the number of configurations that an ensemble may assume, becomes less than unity. Physically, this implies that the number of configurations that the system may have is less than 1, an impossibility since there is always at least 1 configuration: the completely ordered state. Thermodynamically, $W < 1$ obviously implies that the entropy of the ensemble is negative. Flory stated that the classical lattice model yields estimates of the number W of "random" ensemble configurations while precluding the possibility of ordered conformations, thus creating this catastrophe.

The solution to this enigma lies in the boundary conditions employed in formulating the entropy expression. This is most easily observed in the lattice formulations of mixtures of rodlike macromolecules with solvent (holes). Flory's 1956 formulation for a three-dimensional continuum (and succeeding formulations) created an entropy expression containing the degeneracy ω_Θ for rods inclined at an angle Θ from the domain axis:

$$\omega_\Theta = \sigma \sin \Theta \tag{1}$$

Flory determined the rotational degeneracy factor σ by utilizing the following boundary condition: as the ensemble becomes increasingly ordered, the entropy should approach that of the ideal entropy of mixing (one-dimensional *mixing*).

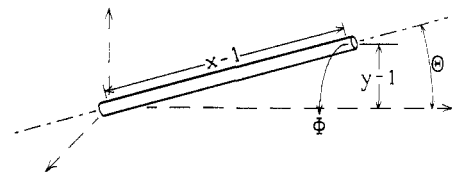

Figure 1. Rod of axis ratio x positioned in three dimensions.

It is possible to position a rod parallel to the domain axis, but a rod inclined at even a small angle from the domain axis has essentially an infinite number of possible rotations around the domain axis compared to the one location available to the perfectly oriented rod. Thus, W for an ensemble of nearly ordered rods is infinitely greater than W for the perfectly aligned case. If the "one-dimensional" case were used as the boundary condition for determining σ, then σ would be on the order of infinity because as $\Theta \to 0$, $\omega_\Theta \to 1$ and thus $\sigma \to \infty$. The absolute entropy values are then always greater than 0. This explanation for the entropy catastrophe holds only for a continuum model and is not valid for systems in which the rods are inclined from or rotated about the domain axis in discrete steps. For the noncontinuous case, the one-dimensional boundary condition is appropriate. Warner described σ as a constant indicative of the system's phase space.[28]

Flory defined the disorientation parameter y in his partition function for rods as the number of submolecules into which the rod is broken in order to fit into the lattice. The relationship of y with x and with the angle of inclination from the domain axis Θ (Figure 1) was described spatially as

$$y - a = b(x - c) \sin \Theta \tag{2}$$

where a, b, and c are constants determined by the model under discussion. Flory's original model used $a = c = 0$ and $b = 1$; this was later altered with $a = c = 0$ and $b = 4/\pi$ by Flory and Ronca.[14] Straley[13] ($a = b = 1$, $c = 0$) and later Warner[16] ($a = c = 1$, $b = 4/\pi$) discussed the merits of a nonvanishing value of y. Results for Flory and Ronca,[14] for Warner,[16] and for $a = b = c = 1$ will be presented here.

Extrema in the rod entropy for a continuous angular distribution first introduced by DiMarzio[11] (and used by Straley[13] and Flory[14,15,21]) give the $(n - 1)$th sine moment f_n as

$$f_n = \int \sin^n \Theta \exp(-\beta(x - c) \sin \Theta)\, d\Theta \tag{3}$$

with $-\beta$ being $\ln [1 - v_x(1 - \langle y \rangle / x)]$. The distribution function P_Θ is

$$P_\Theta = N_{x\Theta}/N_x = (f_1)^{-1} \sin \Theta \exp(-\beta(x - c) \sin \Theta) \tag{4}$$

Entropies are calculated according to eq 16 of Flory and Ronca[14] with the above distribution and with the average value of the disorientation parameter given by

$$\langle y \rangle = a + b(x - c) f_2/f_1 \tag{5}$$

DiMarzio Model

Perhaps the most consistent continuum statistical mechanical model for rigid rods presented to date is that of DiMarzio.[11] It may be summarized as follows. The liquid crystalline domain is composed of N_s spherical solvent molecules of diameter unity and N_x cylindrical solute molecules of length x and diameter unity (axis ratio of x). The total volume of the system is represented by $N = N_s$

+ xN_x. No orientation-dependent interactions nor any internal molecular states are examined.

Because of the importance of the orientational relationships between the rods, an accurate description of the rods' angular bearings becomes necessary. Allow a set of Cartesian coordinates z to be superimposed in some random direction in the ensemble. The spherical variables Θ and Φ will then characterize the relative angular orientations of each of the N_x rods (Figure 1). The angle Θ ($0 \leq \Theta \leq \pi/2$) measures the inclination of a rod from the z_1 axis, and the angle Φ ($0 \leq \Phi < 2\pi$) represents the rotation of this rod about the z_1 axis, as measured from the z_2 axis. The relative angle between the ith and jth rod in the ensemble is denoted as $\epsilon_{i,j}$.

If a large number of rods have been placed into the lattice in a quasirandom manner such that all domain-averaged quantities are approximately their final values and if this number of rods in the lattice is still only a small fraction of the total number N_x, then the total number of ways ν_{j+1} of properly placing the $j+1$ rod into the lattice is given by

$$\nu_{j+1} = \omega_j \frac{(N - jx)^x}{[N - f(x-1)\sum_{\Theta_i} N_{x\Theta_i}(1 - \langle \sin \epsilon_{i,j+1} \rangle)]^{x-1}} \quad (6)$$

where $f = j/N_x$ denotes the fraction of rods that have already been placed into the lattice and the quantity $N_{x\Theta}$ represents the number of rods possessing the specific orientation Θ from the domain axis. The summation in the denominator counts the number of occupied sites projected normal to the direction of the $j+1$ rod when all rods have been placed. In this manner, $\langle \sin \epsilon_{i,j} \rangle$ then represents the average value of the sine between the two orientations Θ_j and Θ_i.

Equation 6 was obtained by specifying z_1 to be the preferred domain axis, if one does indeed exist. Physically, the domain axis actually varies from point to point within the system, the rate of change being dependent upon a variety of parameters including rod volume fraction, dimensionality of the system, rod axis ratio, and the algorithm with which one distinguishes one domain from another (see, for instance, ref 35). The domain is allowed to extend throughout the entire system to eliminate the bias associated with domain determination; all rods with a particular inclination Θ_j are equivalent and thus degenerate by the factor ω_j with respect to one another. As previously discussed, this degeneracy is proportional to $\sin \Theta_j$. The total number of configurations W that the ensemble may assume for a particular distribution of rod angles is then given by

$$W = \prod_j (\nu_j) / \prod_\Theta (N_{x\Theta}!) \quad (7)$$

The entropy of this configuration comes from the logarithm of W:

$$\ln (W)/N = S/Nk = -v_s \ln (v_s) - (v_x/x) \ln (v_x/x) + \int P_j[(1/L_j - r) \ln (1 - rL_j) + (v_x/x) \ln (\omega_{\Theta j}/P_j)] \, d\Theta_j \quad (8)$$

where

$$L_j = 1 - \int P_i \langle \sin \epsilon_{i,j} \rangle \, d\Theta_i \quad (9)$$

$$P_i = N_{x\Theta_i}/N_x \quad (10)$$

and

$$r = v_x(x-1)/x \quad (11)$$

With use of Lagrangian multipliers (or other suitable optimization techniques), the entropy extrema within the interior of the distribution set[11,13] are found to satisfy the following distribution function:

$$P_j = \alpha \sin \Theta_j \exp\left\{ \frac{x}{v_x}\left[\frac{1}{L_j} - r\right] \ln (1 - rL_j) + \frac{x}{v_x}\int \frac{\langle \sin \epsilon_{ij} \rangle}{L_i} P_i \left[\frac{\ln (1 - rL_i)}{L_i} + r\right] d\Theta_i \right\} \quad (12)$$

The parameter α is a normalization factor. Note that the isotropic distribution always satisfies eq 12, regardless of rod axis ratio and volume fraction. The isotropic entropy is given by

$$S/Nk = -v_s \ln v_s - \frac{v_x}{x} \ln \left[\frac{v_x}{\sigma x}\right] + \left[\frac{1}{1 - \pi/4} - r\right] \ln [1 - r(1 - \pi/4)] \quad (13)$$

The chemical potentials are given by

$$(\mu_s - \mu^\circ_s)/kT = \ln (v_s) - \int (P_j/L_j) \ln (1 - rL_j) \, d\Theta_j \quad (14)$$

$$(\mu_x - \mu^\circ_x)/kT = \ln (v_x/x) + \int P_j[((x-1) - x/L_j) \ln (1 - rL_j) + \ln (P_j/\omega_{\Theta j})] \, d\Theta_j \quad (15)$$

The isotropic chemical potentials are then

$$(\mu_s - \mu^\circ_s)/kT = \ln (v_s) - \ln (1 - r(1 - \pi/4))/(1 - \pi/4) \quad (16)$$

$$(\mu_x - \mu^\circ_x)/kT = \ln (v_x/\sigma x) + [x - 1 - x/(1 - \pi/4)] \ln [1 - r(1 - \pi/4)] \quad (17)$$

Rod Distributions and Entropies

DiMarzio showed that when the rods lie along the three principle axis directions, entropy extrema may occur for three different rod distributions: the isotropic phase (equal numbers of rods aligned along the three axes), the nematic phase (all rods aligned along one axis), and a phase in which equal numbers of rods are aligned along two of the axes. A similar situation is found in numerical solutions to eq 12, obtained by a method of successive substitutions of $\{P_j\}$.

The isotropic phase was observed always to satisfy eq 12, regardless of concentration. For more concentrated mixtures of rods, two additional solutions to this equation exist. The first is the nematic phase in which the majority of rods are oriented more or less in the direction of the domain axis. The more accurate term for this distribution is the "positive uniaxial nematic",[30] but it will be referred to here simply as "nematic". The nematic phase order parameters are $\langle \sin \Theta \rangle < \pi/4$ and $s = (3\langle \cos^2 \Theta \rangle - 1)/2 > 0$. The final solution to eq 12 is the negative uniaxial nematic[30] distribution. In this distribution, the majority of rods are oriented much further from the domain axis than in the isotropic phase, such that the probability distribution resembles the form $(\sin \Theta) \exp(\beta \sin \Theta)$, where $\beta > 1$. The order parameters for this phase are $\langle \sin \Theta \rangle > \pi/4$ and $s < 0$. These two solutions of eq 12 are illustrated in Figure 2 for an axis ratio of 100. For the nematic probability distribution, $v_x = 0.105$, $\langle \sin \Theta \rangle = 0.319$, and $s = 0.793$ ($v_x = 0.105$ corresponds to the minimum volume fraction for a stable nematic phase). The negative uniaxial

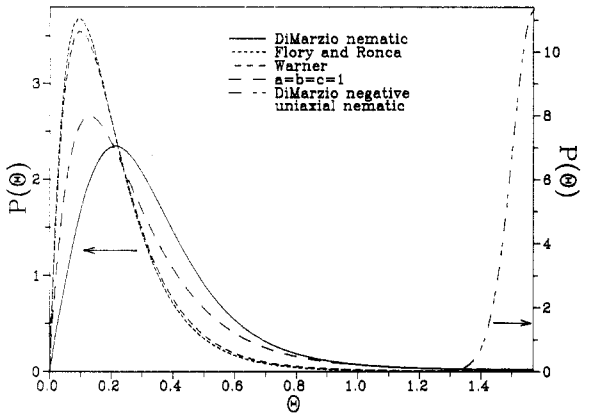

Figure 2. Probability distributions for $x = 100$. Left scale and curves: nematic distributions at $v_x = 0.105$ for DiMarzio (eq 12), Warner,[16] Flory and Ronca,[14] and $a = b = c = 1$. Right scale and curve: DiMarzio negative uniaxial nematic distribution at $v_x = 1$.

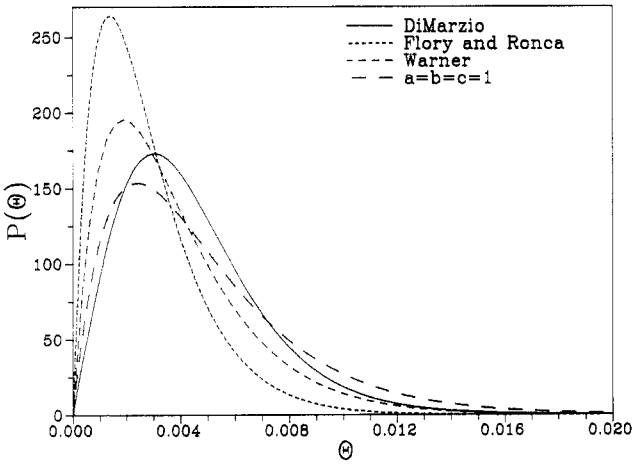

Figure 3. Nematic probability distributions for $x = 100$, $v_x = 1.0$. For DiMarzio (eq 12), Warner,[16] Flory and Ronca,[14] and $a = b = c = 1$.

nematic distribution, calculated for $v_x = 1.0$, has domain-averaged quantities of $\langle \sin \Theta \rangle = 0.997$ and $s = -0.492$.

Also plotted in Figure 2 are probability distributions corresponding to the Flory model for the Flory and Ronca,[14] Warner,[16] and $a = b = c = 1$ rod orientation descriptions for $x = 100$ at $v_x = 0.105$. The Flory model distributions peak before that of DiMarzio, and the $a = b = c = 1$ distribution estimates that of DiMarzio the best. Calculations have shown that Flory models with $b = 4/\pi$ also yield negative uniaxial nematic solutions to the distribution function for the concentrated regime. Figure 3 illustrates that for a neat system of $x = 100$ rods, the Flory models again reach their maximum before the DiMarzio model. At this volume fraction, the two nonvanishing y models ($a = 1$) approximate the distribution of DiMarzio more closely than the vanishing y model. The DiMarzio distribution always peaks at a higher angle than do the Flory models because it is more difficult to pack parallel submolecules into the Flory lattice-derived continuum than it is to insert unbroken rods into the DiMarzio continuum.

The dependence of $\langle \sin \Theta \rangle$ on volume fraction for the two DiMarzio anisotropic phases is depicted in Figure 4 for an axis ratio of 100. As the rod volume fraction decreases, the order of the anisotropic phases decreases slowly until $v_x \approx 0.25$, where the order decreases dramatically with decreasing rod volume fraction. The $\langle \sin \Theta \rangle$ for $a = b = c = 1$ is also shown in Figure 4. This distribution always possesses orientations which approximate those of DiMarzio better than the Warner or the Flory and Ronca models. The description suggested by Straley ($a = b = 1$, $c = 0$)[13] follows the $a = b = c = 1$ distribution quite closely when $x \gg 1$.

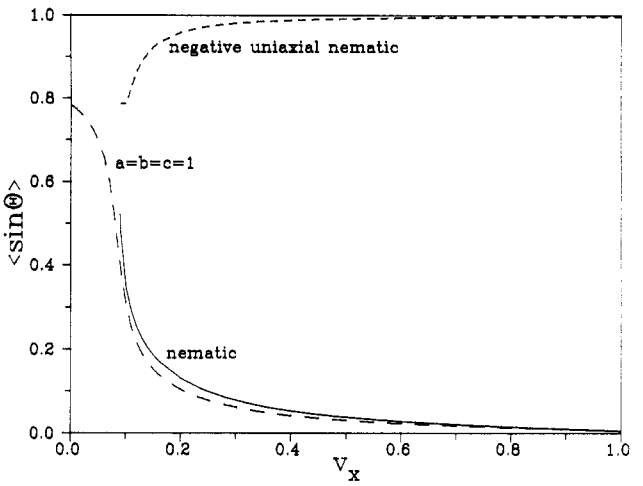

Figure 4. Domain-averaged quantity $\langle \sin \Theta \rangle$ as a function of v_x for $x = 100$. Nematic and negative uniaxial nematic values obtained by use of eq 12; $a = b = c = 1$ values (nematic) from eq 4 and 5.

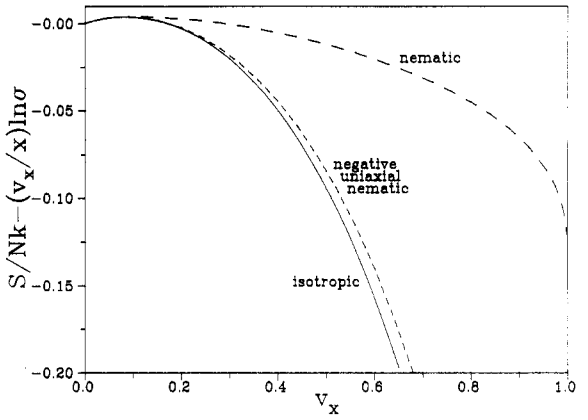

Figure 5. Relative DiMarzio entropies for $x = 100$. Isotropic entropy from eq 13 and the two anisotropic entropies from eq 8 and 12.

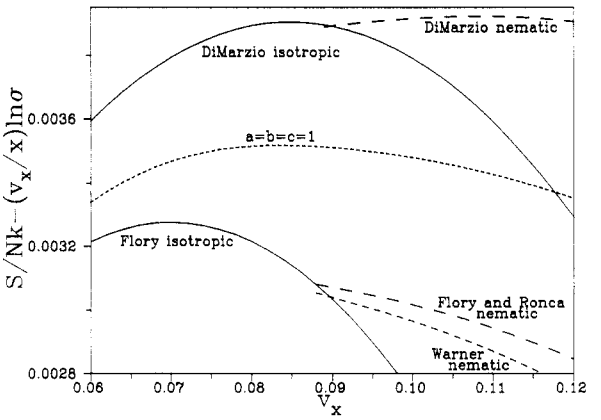

Figure 6. Entropies at the transition for rods of $x = 100$. Upper two curves are DiMarzio isotropic and nematic entropies. Lower four curves are entropies for various Flory models.

The negative uniaxial nematic distribution never maximizes the configurational entropy (Figure 5) for the molecular interactions considered. The negative uniaxial nematic distribution is an entropy extremum for $v_x > 0.09$, and its entropy always lies between those of the nematic

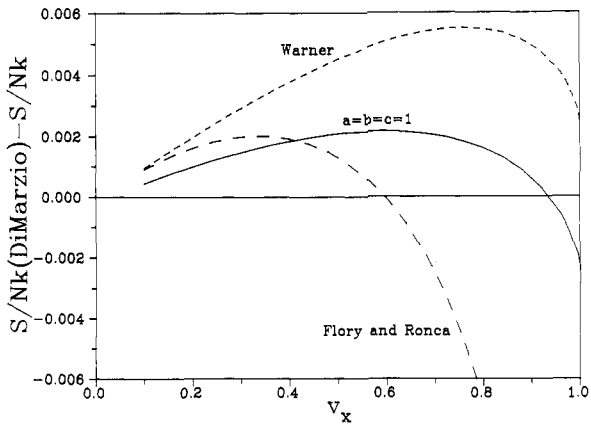

Figure 7. Difference between DiMarzio and entropy and entropies of the Flory models.

and the isotropic phases. The maximization of the entropy by the isotropic phase[2] at lower rod concentrations is better depicted in the upper two curves of Figure 6. The nematic entropy line is truncated for $v_x < 0.089$ because the nematic phase is not a solution to eq 12 below this volume fraction. The nematic entropy always crosses the isotropic entropy, thus complying with the thermodynamic phase rules. The negative uniaxial nematic phase is not depicted in this graph; its entropy lies virtually on top of the isotropic entropy for the concentrations plotted in Figure 6.

Figure 6 also contains entropies for the previously discussed Flory models in this first-order transition region. For this concentration range, all isotropic and nematic Flory model entropies are lower than the corresponding DiMarzio entropies. Because the Flory and Ronca theory and the Warner modification possess very similar rod distributions at lower rod concentrations, their nematic entropies are quite similar in this concentration range. Note that both the sign and the magnitude of the entropy change at the transition are quite different for the DiMarzio and the Flory models. The $a = b = c = 1$ model always gives a nematic phase at maximized entropy, so that it experience no isotropic–nematic transition (see, for instance, ref 13). Regardless, this entropy lies closer to the DiMarzio nematic entropy than the other two (Figure 7). The equation for the Flory and DiMarzio entropies have the same form (ideal mixing of polymer and solvent plus an orientational term), but calculations have shown the Flory model to be much more sensitive to the actual rod distribution than the DiMarzio model. The DiMarzio entropy then has a much broader entropy maximum in $\{P_j\}$ space than the Flory model. Note the difference in the three Flory model entropies. Substitution of the $a = b = c = 1$ orientation function into the DiMarzio entropy (eq 8) yields entropies which are virtually indistinguishable from those calculated with the DiMarzio distribution. With the DiMarzio model as a standard, the Warner entropy consistently underestimates the entropy more than the $a = b = c = 1$ model. At lower concentrations, even the Flory and Ronca model comes closer to the DiMarzio entropy than does the Warner model, but at higher rod volume fractions the Flory and Ronca model severely overestimates the entropy because of the miscounting of y at these high concentrations.

For a neat system of rods, the obvious minimum in the entropy is the crystalline state. Because of the domain-averaging techniques employed in the derivations presented, orders of the smectic type are not counted, thus eliminating the $S = 0$ configuration. Likewise, this domain averaging disallows cholesteric phases and other local orderings.[29] The minimum entropy for the Flory and DiMarzio derivations is that of the perfectly ordered nematic state. In general, this distribution will not satisfy eq 12 because $\partial S/\partial P_j \neq 0$: $\partial S/\partial P_j = \infty$ and $-\infty$ for $\Theta_j \neq 0$ and $\Theta_j = 0$, respectively (this distribution also lies on the boundary of the $\{P_j\}$ distribution set). In the limit as $x \to \infty$, the distribution for the entropy maximum approaches that of the completely ordered nematic for $v_x > 0$ (a cholesteric configuration of rods would have a higher entropy).

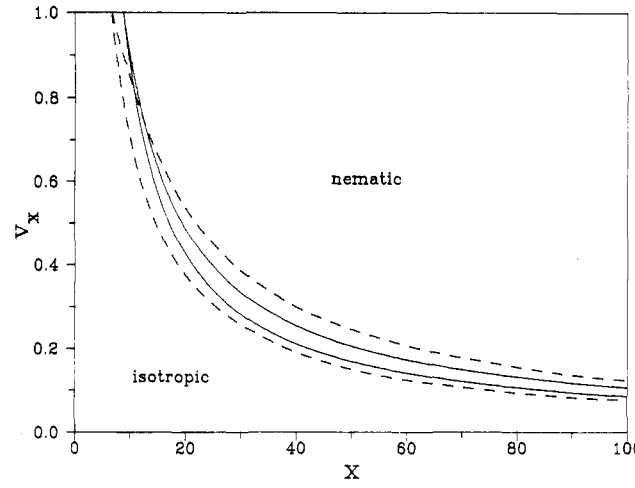

Figure 8. Athermal phase equilibria for $x = 100$. Solid lines represent equilibria determined from eq 14–17. Dashed lines from Flory.[9]

Straley demonstrated that the isotropic distribution never maximized the Flory entropy except as $v_x \to 0$. He also noted the inconsistency in the definition of the disorientation parameter y and suggested a more accurate description, showing that improving the disorientation parameter description still led to a nematic phase being the more stable. Recall that in the DiMarzio approach, where the preferred axis was specified prior to the process of rod distribution, the resulting isotropic entropy was greater than the nematic entropy, except for very concentrated solutions.

Equating species' chemical potentials (eq 14–17) in different phases yields phase equilibria. Figure 8 supports the accepted[2,9,30] conclusion that the anisotropy of the rods creates a first-order phase separation above a critical concentration. The solid lines represent the isotropic–nematic phase equilibria computed according to the DiMarzio approach. To the right of the two solid lines lies the nematic phase. Between the two solid lines is the two-phase region, and the isotropic phase is to the left of the two solid lines. The dashed lines depict equilibria calculated by the original 1956 Flory approach, with similar phases. To within experimentally measured x and v_x, these models are quite similar. Phase equilibria for the Flory and Ronca[14] and for the Warner[16] models have narrower biphasic regions and lie much closer to the DiMarzio model than to the Flory 1956 model.

Data describing various equilibria for the models discussed are shown in Table I. The critical data (transition at $v_x = 1$) for the Warner and for the Flory and Ronca models show that the Warner model comes close to estimating the DiMarzio critical rod axis ratio, but the nematic phase orientations at the transition are quite far off for both Flory models. The phase transition for $x = 100$ shows a similar case: the Flory models come close to the DiMarzio model in estimating the rod volume fraction at the transition but are very far off in describing nematic orientation. Domain-averaged values from Figures 2 and 3 are also tabulated ($x = 100$; $v_x = 1$ and 0.105), quantifying the difference in the Flory and DiMarzio models. These

Table I
Comparison of the Athermal Rod Volume Fractions and Order Parameters for Various Models[a]

	DiMarzio	Warner	Flory and Ronca	$a = b = c = 1$
crit values				
x_c	8.83	8.75	6.42	
s_c	0.794	0.922	0.947	
$\langle \sin \Theta \rangle_c$	0.315	0.185	0.152	
$x = 100$				
$v_{x,iso}$	0.0841	0.0795	0.0776	
$v_{x,nem}$	0.105	0.113	0.113	
s_{nem}	0.793	0.925	0.929	
$\langle \sin \Theta \rangle_{nem}$	0.319	0.181	0.177	
$x = 100$, $v_x = 0.105$				
s	0.793	0.901	0.909	0.825
$\langle \sin \Theta \rangle$	0.319	0.208	0.201	0.278
$x = 100$, $v_x = 1$				
$\langle \sin \Theta \rangle$	0.00442	0.00376	0.00278	0.00479

[a] First three rows represent critical ($v_x = 1$) values of x, $s = (3\langle \cos^2 \Theta \rangle - 1)/2$, and $\langle \sin \Theta \rangle$. Middle four rows are phase transitions for $x = 100$ rods. The last three rows give orientation parameters for $x = 100$ rods at $v_x = 0.105$ and 1.

values show that the $a = b = c = 1$ description estimates the DiMarzio distributions the best. Interestingly, in a derivation quite similar to that of DiMarzio but made more tractable,[28] Warner reported that $x_c = 8.98$ and $s_c = 0.831$.

It has been demonstrated experimentally that the Flory lattice model for rigid rods gives a better prediction of the incipience of phase separation than do other models[36] (within the complication of effective axis ratios and persistence lengths[8]), though experimental evidence also suggests that at near athermal conditions, the biphasic gap should be narrower than that predicted by the Flory model.[10,37] The Flory two-phase region is considerably wider than the DiMarzio approach because of the miscalculation of both the isotropic and nematic thermodynamic quantities. For axis ratios less than 8.83, only the isotropic phase exists at athermal conditions in the DiMarzio approach. The nematic order parameters at the incipience of phase separation remain fairly constant at $\langle \sin \Theta \rangle \approx 0.32$ and $s \approx 0.79$ over a wide range of axis ratios. This result is similar to that obtained by the virial expansion method of Onsager,[2,5] though the volume fractions at phase separation are quite dissimilar.[13] Alben's statistical mechanical theory of rodlike particles[12] was demonstrated to exhibit athermal phase relationships more similar to those of Onsager[2] than of DiMarzio.

Recall that in these approaches the isotropic and nematic entropies cross. Thus, when simple intermolecular interactions are considered in the form of the χ interaction parameter,[9,38] the isotropic–nematic two-phase region should narrow as χ decreases (disregarding polyelectrolytic effects[7,8]).

Concluding Remarks

The statistical mechanical approach of DiMarzio for packing rigid rodlike particles in a nonoverlapping fashion has been shown to be fairly self-consistent and should be more accurate than the method of Flory. The thermodynamic equations derived from DiMarzio's approach yielded results that manifest, with the exception of ease of execution, the desirable attributes of previous models. This rigorous approach preserves the agreement with experimentally observed isotropic–nematic phase relationships.

For concentrated rod solutions, several different extremes in the entropy equation were found, with the nematic rod distribution maximizing the entropy in this regime. The negative uniaxial nematic rod distribution also is a local extreme in the entropy equation for concentrated solutions, and it possesses a higher entropy than the disordered distribution. Throughout the entire concentration range, the isotropic distribution is a local entropy extreme. The isotropic domain maximizes the dilute solution entropy, and the perfectly oriented domain always minimizes the entropy for finite x.

Flory's generalization from a lattice to a continuum was not complete in his use of the one-dimensional boundary condition to determine σ. Though inconsequential in phase equilibria determinations, this condition yielded negative absolute entropies, creating the so-called entropy catastrophe. It had previously been argued[12,31] that the Flory lattice derivation for rods did not include certain highly ordered distributions, therefore causing the catastrophe. A quick inspection of the DiMarzio rigid rod partition function will convince one that all longitudinally disordered rod ensemble configurations, from highly ordered to entirely disordered, are considered. Indeed, even the Flory approach included the perfectly oriented phase in its calculations. The perfectly ordered phase possesses a very low entropy in a three-dimensional continuum due to the rotational degeneracy factor σ and thus will not maximize the entropy except in the case where $x \to \infty$ and $v_x \to 1$. The entropy catastrophe is thus shown to be nonexistent for the case of rigid rods.

The Flory models yield rod distributions similar to that of the more accurate DiMarzio model. As a consequence of the lattice derivation, the Flory distributions peak at a lower angle of inclination than the DiMarzio distribution. The Flory $a = b = c = 1$ distribution and entropy mimic those of DiMarzio most consistently, though this entropy cannot be used for any equilibria determinations. Because the DiMarzio entropy in $\{P_j\}$ space is somewhat broad, the $a = b = c = 1$ distribution can be used in the DiMarzio entropy equation qute readily to yield highly accurate entropies with considerably less computational effort. The $b = 4/\pi$ rod descriptions give phase equilibria which become closer to those of DiMarzio as x increases but which do not describe the nematic phase rod orientations at the transition and higher rod volume fractions.

Acknowledgment. We thank the Office of Naval Research Chemistry Program for support of this work.

References and Notes

(1) Chandrasekhar, S. *Liquid Crystals*; Cambridge University Press: New York; 1977; Chapter 1.
(2) Onsager, L. *Ann. N. Y. Acad. Sci.* **1949**, *51*, 627.
(3) Isihara, A. *J. Chem. Phys.* **1951**, *19*, 1142.
(4) Zwanzig, R. *J. Chem. Phys.* **1963**, *39*, 1714.
(5) Lasher, G. *J. Chem. Phys.* **1970**, *53*, 4141.
(6) Straley, J. P. *Mol. Cryst. Liq. Cryst.* **1973**, *24*, 7.
(7) Stroobants, A.; Lekkerkerker, H. N. W. *Macromolecules* **1986**, *19*, 2232.
(8) Odijk, Th. *Macromolecules* **1986**, *19*, 2313.
(9) Flory, P. J. *Proc. R. Soc. London, A* **1956**, *234*, 73.
(10) Miller, W. G.; Wu, C. C.; Wee, E. L.; Santee, G. L.; Rai, J. H.; Goebel, K. G. *Pure Appl. Chem.* **1974**, *38*, 37.
(11) DiMarzio, E. A. *J. Chem. Phys.* **1961**, *35*, 658.
(12) Alben, R. *Mol. Cryst. Liq. Cryst.* **1971**, *13*, 193.
(13) Straley, J. P. *Mol. Cryst. Liq. Cryst.* **1973**, *22*, 333.
(14) Flory, P. J.; Ronca, G. *Mol. Cryst. Liq. Cryst.* **1979**, *54*, 289.
(15) Flory, P. J.; Ronca, G. *Mol. Cryst. Liq. Cryst.* **1979**, *54*, 311.
(16) Warner, M. *Mol. Cryst. Liq. Cryst.* **1982**, *80*, 67.
(17) Flory, P. J.; Abe, A. *Macromolecules* **1978**, *11*, 1119.
(18) Abe, A.; Flory, P. J. *Macromolecules* **1978**, *11*, 1122.
(19) Flory, P. J.; Frost, R. S. *Macromolecules* **1978**, *11*, 1126.
(20) Frost, R. S.; Flory, P. J. *Macromolecules* **1978**, *11*, 1134.
(21) Warner, M.; Flory, P. J. *J. Chem. Phys.* **1980**, *73*, 6327.
(22) Moscicki, J. K. *J. Polym. Sci., Polym. Phys. Ed.* **1985**, *23*, 327.
(23) Flory, P. J. *Macromolecules* **1978**, *11*, 1138.
(24) Flory, P. J. *Macromolecules* **1978**, *11*, 1141.
(25) McCrakin, F. L. *J. Chem. Phys.* **1978**, *69*, 5419.
(26) Sikorski, A.; Orszagh, A. *Mol. Phys.* **1985**, *55*, 363.
(27) Boehm, R. E.; Martire, D. E. *Mol. Phys.* **1978**, *36*, 1.

(28) Warner, M. *Mol. Cryst. Liq. Cryst.* **1982**, *80*, 79.
(29) Bawendi, M. G.; Freed, K. F. *J. Chem. Phys.* **1986**, *85*, 3007 and references therein.
(30) Gramsbergen, E. F.; Longa, L.; de Jeu, W. H. *Phys. Rep.* **1986**, *135*, 195.
(31) Flory, P. J. *Proc. Natl. Acad. Sci. U.S.A.* **1982**, *79*, 4510.
(32) Romanko, W. R. Master's Thesis, Northwestern University, 1987.
(33) Gujrati, P. D. *J. Phys. A: Math. Gen.* **1980**, *13*, 437.
(34) Gujrati, P. D.; Goldstein, M. *J. Chem. Phys.* **1981**, *74*, 2596.
(35) Baumgartner, A. *J. Chem. Phys.* **1986**, *84*, 1905.
(36) Flory, P. J. *Adv. Polym. Sci.* **1984**, *59*, 1.
(37) Ballauff, M.; Flory, P. J. *Ber. Bunsen-Ges. Phys. Chem.* **1984**, *88*, 530.
(38) Flory, P. J. *Principles of Polymer Chemistry*; Cornell University Press: Ithaca, NY, 1953.

Junction Fluctuations in Confined Chain Models of Rubber Elasticity

Douglas Adolf

Sandia National Laboratories, Albuquerque, New Mexico 87185.
Received November 14, 1987; Revised Manuscript Received February 5, 1988

ABSTRACT: The junction fluctuations in a micronetwork of entangled chains are examined and compared to the assumptions made by the constrained junction theories. The entanglements acting on the micronetwork chains are pictured as hoops of infinitesimal diameter through which a chain must pass. Over a limited range of the uniaxial extension ratio, the calculated fluctuations qualitatively agree with the constrained junction theories. Quantitative agreement is improved by allowing the hoops to have finite size. However, junction fluctuations are seen to have little effect on the uniaxial force of the micronetwork. The force is dominated by the strain dependence of the chain entropy. This implies that agreement in the junction fluctuations is not sufficient to infer that the constrained junction theories correctly model the primary effects of entanglements on network chains.

Introduction

All theories for the equilibrium elasticity of polymer networks rest on the assumption that the elastic force is primarily due to the change in entropy with strain of the covalently bonded network chains and that the noncovalent forces simply determine the isotropic pressure of the system.[1] To determine the force, then, one needs the probability distribution for the end-to-end vector for a network chain and the connectivity of the network itself. The simplest approach to rubber elasticity is to assume that the network is composed of Gaussian chains that are able to pass through each other freely and that the network junctions are fixed at their mean positions. This is the basis of the affine theory of rubber elasticity.[2] James and Guth[3] modified this approach to allow some of the network junctions to fluctuate in a self-consistent fashion (the phantom network theory). The force in response to uniaxial deformation for both of these theories is of the form $f \sim (\lambda - 1/\lambda^2)$, where λ is the uniaxial extension ratio. However, it is well-known that this strain dependence is incorrect for networks with chains of sufficient length.[1] The reduced force, $[f^*] = f/(\lambda - 1/\lambda^2)$, actually decreases with increasing extension ratio.

Modern theories attribute this strain dependence of the reduced force to entanglements that conserve network topology. Conserving topology exactly would result in an extremely difficult many-body problem, so the usual approach is to assume that each chain (or junction) is affected by entanglements in an average and independent fashion. The theories differ in how they model the effect of entanglements. One class of theories,[4,5] the constrained junction theories, assumes that the major effect of entanglements is to modify the network junction fluctuations. In the phantom network theory, the junction fluctuations are strain independent, whereas in the constrained junction theories, the fluctuations are assumed to be strain dependent. The chain statistics, however, are still assumed to be Gaussian, so the strain dependence of the reduced force is determined by the assumed strain dependence of the junction fluctuations. The other class of theories, the confined chain models, assume that the entanglements affect the entire chain. The effects of entanglements along the chain have been modeled as confining tubes,[6,7] slip-links,[8] and hoops through which the chain must pass.[9] In these theories, the fluctuations of the network junctions are neglected, so the strain dependence of the reduced force is dominated by the effect of the entanglements on the chain entropy.

In this paper, we are interested in the magnitude and strain dependence of the junction fluctuations for a finite-sized network composed of entangled chains using one type of confined chain model, the hoop model.[9] From this, we can determine if the assumed strain dependence of the junction fluctuations in the constrained junction theories is consistent with the predictions of this confined chain model. More importantly, we can see which effect of entanglements, that affecting chain entropy or junction fluctuations, dominates the reduced force.

Model and Theory

The hoop model envisions entanglements as hoops through which the polymer chain must pass. In general, these hoops may be of arbitrary size and placement. However, a simple analytical result is obtained only in the limit as the hoop diameter vanishes. We have previously shown,[9] that the partition function for such a chain with arbitrarily placed hoops is given by

$$Q = \frac{\sum_1^M t_i}{\prod_1^M t_i} \exp\left(-\frac{3}{2Nl^2}\sum_1^M t_i^2\right) \qquad (1)$$

where N is the number of segments each of length l on a

0024-9297/88/2221-2249$01.50/0